Laser-induced damage measurements in CdTe and other II–VI materials

M. J. Soileau, William E. Williams, Eric W. Van Stryland, and M. A. Woodall

Results of laser-induced damage measurements in CdTe and other selected II–VI materials are reported. These studies were conducted using pulsed 1.06-μm radiation from a Nd:YAG laser. The laser pulse width was varied from ~40 to 9000 psec (9 nsec). The laser-induced surface breakdown irradiance measured for CdTe over this pulse width range scaled as $t_p^{-1/2}$ [t_p is the laser pulse width (FWHM)]. This indicates that laser-induced damage in this material is due to linear absorption by a thin surface contamination layer.

I. Introduction

The II–VI compounds and various single element semiconductors are used as window materials for continuous output lasers operating in the 10.6-μm region. These materials are also used as the high index of refraction component of multilayer dielectric coatings for laser and other infrared optics applications. While these materials have proved useful for nonlaser infrared applications and for many continuous output laser applications, they are generally avoided in pulsed laser systems.

There are a variety of fundamental reasons to avoid the high index materials for pulsed laser applications. The high index means very high Fresnel losses at interfaces, and the field enhancement associated with surface scratches and other defects[1,2] is more pronounced. Bettis *et al.*[3] have argued that high index materials will have lower damage thresholds based on local field considerations. Finally, Wang's rule[4] for nonlinear indices of refraction, n_2, implies that a material with a large linear index will also have a large n_2, and thus the problems associated with self-focusing will be most pronounced for high index materials.

Despite these problems there are a variety of pulsed laser applications which require the use of the II–VI compounds, e.g., a system that has optics which are shared by lasers of different frequencies and different pulse widths. These materials are also of interest in integrated optics and phase conjugation; two applications for which a large nonlinear index of refraction is advantageous. In any such application it is important to know the operating limits set by laser-induced damage to the materials.

The authors are with North Texas State University, Center for Applied Quantum Electronics, Physics Department, Denton, Texas 76203.

Received 17 July 1982.
0003-6935/82/224059-04$01.00/0.

In this study we measured the pulsed laser-induced surface damage threshold of CdTe, ZnSe, CdS, and ZnTe at 1.06 μm. The study emphasized CdTe because of its use as a pulse shaping device[5] in laser fusion systems and other applications and because it is a good model system for use in studying nonlinear absorption. The band gap in CdTe is 1.32 eV, which lies between 1.06 and 0.53 μm. The position of the band gap in CdTe means that it is transparent to 1.06-μm radiation but has a relatively large two-photon absorption coefficient. These experiments show that absorption in CdTe is dominated by two-photon absorption and absorption by the two-photon generated excess carriers at 1.06 μm near the damage threshold. However, the surface damage threshold irradiance scales as $t_p^{-1/2}$ (t_p is the laser pulse width) which is characteristic of damage due to surface contamination.

II. Experimental

The laser source for the picosecond studies was a passively mode-locked microprocessor-controlled[6] Nd:YAG laser system operating at 1.06 μm. A single pulse of measured Gaussian spatial and temporal pulse shapes was switched from the mode-locked train and amplified. The temporal pulse width was variable between 30 and 200 psec [full widths at half-maximum (FWHM)] by selecting various etalons as the output coupler. The width of each pulse was monitored by measuring the ratio R of the square of the energy in the fundamental (1.06 μm) to the energy in the second harmonic, produced in a $LiIO_3$ crystal. This ratio is directly proportional to the laser pulse width as long as the spatial profile remains unchanged.[7] The ratio was calibrated by measuring the pulse width using type-I second-harmonic autocorrelation scans. The observed three-to-one signal-to-background ratios indicated clean mode locking.[8] To ensure that the ratio R is proportional to the pulse width and provides a valid pulse width monitor, scans were performed for all output coupler etalons.

The laser beam was focused onto the sample surface with a single element lens of best form design, i.e., designed for minimum spherical aberrations. The focal

Reprinted from **APPLIED OPTICS**, Vol. 21, page 4059, November 15, 1982

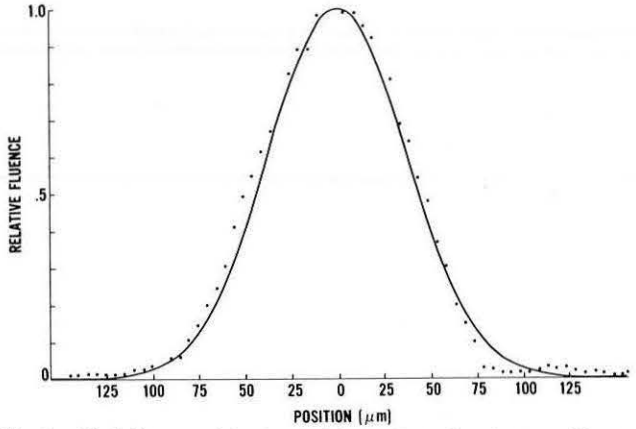

Fig. 1. Pinhole scan of the focused beam from the picosecond laser. The dots are the actual data points and the solid line is an ideal Gaussian of width 77 μm. After correction for the finite size of the pinhole used to make this scan the focused beam radius was determined as 75 ± 5 μm.

position (547 ± 2 mm from the lens mechanical center) was determined by a series of pinhole scans at various distances from the focusing lens. The $1/e^2$ radius of the irradiance of the unfocused beam was 2.35 mm resulting in an $f/116$ imaging system. The focal radius at the $1/e^2$ point of the irradiance was 75 ± 3 μm as determined by pinhole scans. Figure 1 is a plot of the beam scan data and a Gaussian best fit to the data. Some of the data were taken with the sample at the focal position and some data were taken with the specimen 2.70-cm behind the focal point. The beam radius was calculated using Gaussian optics to be 139 ± 4 μm at a position 2.70-cm behind focus. The beam was not scanned at this position, however; it was scanned at 2.25-cm behind focus. The measured radius at this position was 122 ± 7 μm, which is within 5% of the 116-μm value predicted by Gaussian optics.

The beam irradiance was controlled by varying the voltage in the amplifier stage of the laser. Beam scans were conducted at various amplifier settings thereby verifying that the beam spatial profile was unchanged over the range of amplifier settings used. The pulse energy into the specimen and transmitted through the specimen was monitored for each laser shot.

A piezoelectric transducer was mounted on the samples using pressure contact. The transducer was used to monitor the acoustic signal generated in the sample by linear and nonlinear absorption of light by the sample. The optoacoustic technique used in this experiment is described elsewhere.[9] The optoacoustic signal and the transmission of the sample were monitored as the laser output was increased to a value which produced damage. In this experiment damage was taken to be any perceptible change in the same as viewed with a 20× microscope. The results of the nonlinear absorption measurements are discussed in detail in Ref. 10. The nanosecond data were taken using a Q-switched Nd:YAG laser operating at 1.06 μm. The pulse width for this device was 9-nsec (FWHM) as measured using a high speed photodiode read by a 1-GHz bandwidth oscilloscope. The focal radius of the Q-switched beam at the sample surface was 26 μm as calculated using Gaussian optics and the measured unfocused beam parameters. This laser system is described more completely elsewhere.[11]

The CdS and ZnTe samples were single crystals. The CdTe was large grain-size polycrystalline material grown by chemical vapor deposition.[12]

III. Results and Discussions

The results of the picosecond surface damage measurements are summarized in Table I. The threshold values given are the peak irradiance levels, I_B, which produce damage 50% of the time as determined using the procedure described by Porteus *et al.*[13] In all the picosecond measurements the pulsewidth of each shot was measured and the irradiance calculated. Only shots within the pulse width range shown in Table I were used in determining the damage thresholds.

The laser-induced damage observed in this work always occurred on the front or entrance surface. The imaging lens for the picosecond measurements was used at $f/116$. This means that the depth of focus was very large and thus the beam radius was approximately the same at the front and exit surfaces. For this situation (neglecting absorption) the local electric field of the light beam at the rear surface is larger than that at the front surface by a factor $2n/(n+1)$, where n is the index of refraction of the specimen.[14] Thus, the exit surface should fail at irradiance levels $4n^2/(n+1)^2$ lower than the front surface. For CdTe this factor is ~2.3 and thus the exit surface should fail at irradiance levels equal to ~0.43 times the front surface damage threshold.

Table I. Surface Damage Threshold Data

Material	Surface Damage Threshold Irradiance (GW/cm^2) Focal Radius ($1/e^2$ Point of the Irradiance)		
	139 μm	75 μm	26 μm
CdTe	a) 1.24 ± 0.04 t_p = 124 ± 10 ps b) 1.18 ± 0.06 t_p = 108 ± 10 ps c) 2.06 ± 0.10 t_p = 46 ± 5 ps	a) 0.82 ± 0.03 t_p = 188 ± 15 ps b) 1.96 ± 0.10 t_p = 42 ± 3 ps	0.10 ± 0.01 t_p = 9000 ± 500 ps
ZnTe	0.43 ± 0.03 t_p = 46 ± 5 ps		
ZnSe		a) 12.4 ± 0.9 t_p = 41 ± 3 ps b) 14.9 ± 1.5 t_p = 34 ± 3 ps	
CdS		20 ± 0.6 t_p = 35 ± 3 ps	

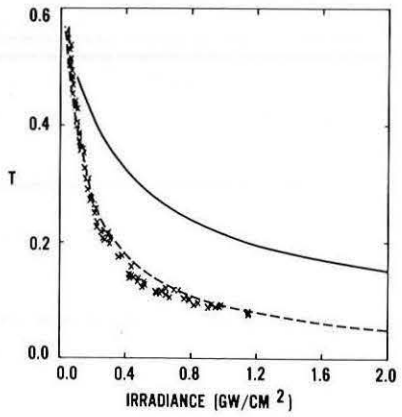

Fig. 2. Nonlinear absorption in CdTe. Here the transmission of ~150-psec (FWHM) 1.06-μm pulses is plotted as a function of the input irradiance. The solid line is the theoretical curve for two-photon absorption. The dashed line is a fit including the absorption by photogenerated carriers using a two-photon absorption coefficient of 35 cm/GW and a carrier absorption cross section of 2×10^{-16} cm^2. The zero irradiance transmittance of this CdTe sample at 1.06 μm is 0.63 and is determined by the Fresnel reflection losses at the sample surface.

The fact that front surface damage precedes exit surface damage in these experiments can be understood in terms of the nonlinear absorption which preceeds damage in the material studied. Figure 2 is a plot of the transmission as a function of incident irradiance for CdTe. The laser pulse width for these data was ~150 psec. The points are actual data and the solid line the theoretical prediction based on two-photon absorption.[10,15–17] The dashed line is a theoretical fit including the effects of photogenerated carriers with a two-photon absorption coefficient of 35 cm/GW and an overall excess carrier absorption cross section of 2×10^{-16} cm^2.[10] The intercept (zero intensity) corresponds to the Fresnel losses and small linear absorption losses. Note that the transmission at 0.4 GW/cm^2 is down by more than a factor of 5 or ~2.5 times the loss due to Fresnel reflections and linear absorption. This means that, for intensities of 0.4 GW/cm^2 and above, the field enhancement at the exit surface will be negated by the high nonlinear absorption. Note that the measured damage threshold for the front surface was ~1.2 GW/cm^2 for this pulse width and thus the nonlinear absorption reduced the flux at the rear surface to a value below the measured front surface threshold. The nonlinear absorption data are discussed in greater detail in Ref. 10. The presence of the photogenerated carriers can further reduce the intensity at the rear surface by plasma defocusing[18–20] although for these thin samples such an effect is negligible.

Nonlinear transmission and nonlinear optoacoustic measurements were made for all the materials listed in Table I. Absorption in CdTe and ZnTe was dominated by two-photon absorption and subsequent photogenerated carrier absorption, and absorption in CdS and ZnSe was dominated by three-photon absorption and subsequent photogenerated carrier absorption.[10] While the absorption in these specimens was dominated by multiphoton processes, damage appeared to be due to linear absorption caused by surface defects and/or surface contamination as the following analysis shows.

The data in Table I indicate that the surface damage threshold for CdTe with 40-psec pulses is independent of the focal radius to within the uncertainty of the measurement. Bettis *et al.*[21] have used a variety of surface damage threshold data to derive a scaling law which predicts that the surface damage threshold irradiance of dielectrics scales as $1/w$, where w is the focal radius. However, their model is based on the spatial spreading of a laser-induced plasma and no plasma was observed in these experiments (i.e., no visible flash was observed upon damage in a darkened room). Examination of the damage sites and the observed pulse width dependence both indicate that damage in these materials was associated with surface defects and contamination. We attribute the lack of spot size dependence to the fact that surfaces have a relatively high density of defects which initiate the damage, and thus the probability of finding a defect within the beam radius is essentially unity for the smallest spot size used (26-μm radius).

The CdTe data in Table I are plotted in Fig. 3. The solid line in Fig. 3 is a least-squares fit of the data to a $t_p^{-1/2}$ dependence. Note that the fit to the data is very good over the entire 40–9000-psec range. The I_B dependence on the laser pulse width t_p can be understood in terms of a simple thermal failure model. Suppose that there is a thin absorbing layer on the surface and damage is initiated by raising the temperature of this layer to a value which results in melting or an irreversible phase change which changes the surface appearance. If such a layer has a thickness δ which is less than the thermal diffusion depth (i.e., $\delta < \sqrt{t_p \rho}$, where ρ = thermal diffusivity of the material and t_p is the laser pulse width), heat is lost from the irradiated area during the laser pulse. The net result is that more energy is

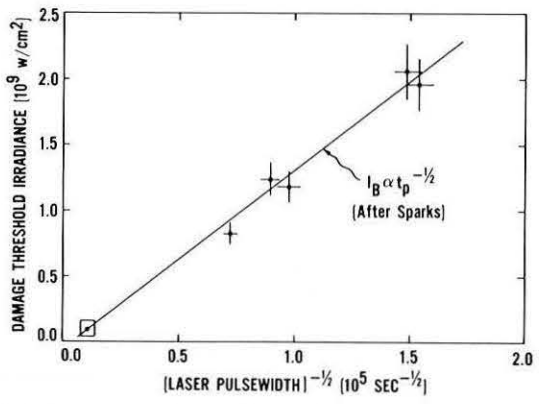

Fig. 3. Front surface damage threshold irradiance for CdTe vs $t_p^{-1/2}$. The irradiance is given in GW/cm^2, and $t_p^{-1/2}$ is in units of 10^5 sec$^{-1/2}$. The solid line is the least-squares fit of the data to a $t_p^{-1/2}$ dependence (t_p is the laser pulse width, FWHM). All the data were taken with Nd:YAG lasers operating at 1.06 μm. The box around the data point on the lower left is added for emphasis and does not correspond to the experimental uncertainty of this point (which is within the size of the data point because of the scale used here).

required to raise the surface temperature a given amount for relatively long pulses than for relatively short pulses. One-dimensional heat transfer calculations (diffusion along the radius of these relatively large spots can be ignored) indicate that the threshold energy density should scale as $t_p^{1/2}$ and the threshold irradiance should scale as $t_p^{-1/2}$.

Sparks and Duthler[22] have modeled thermal damage due to surface inclusions. Their solution to the heat transport equation predicts that $I_B \propto t_p^{-1/2}$ for the case of metallic inclusions for which the absorption skin depth is much less than the thermal diffusion depth. Their model assumes that the skin depth is much less than the inclusion radius and treats absorption by spherical inclusions the same as absorption by a plane slab with a δ-function source. Thus, this model should work equally well for absorption by a thin contamination layer (such as an oxide layer 10–100 Å thick). The fact that the $t_p^{-1/2}$dependence is seen for pulses as short as 42 psec indicates that the absorption which leads to damage occurs in a layer of thickness $\delta \lesssim 2000$ Å thick. Such absorption could be due to metallic inclusions or a thin surface contamination layer. Further evidence for the dominant role of surface contamination was the fact that chemical etching of the CdTe raised its surface damage threshold from 2 to 5.8 GW/cm^2 for 40-p-sec pulses.

A final observation regarding these measurements is that we observed visible light emission from the CdS and ZnSe samples prior to damage. This visible light was emitted in the forward direction and was fairly well collimated. Spectral analysis of the emission from ZnSe revealed that the light was monochromatic and the wavelength was within 1 Å (the limit of our spectrometer resolution) of frequency doubled 1.06 μm, i.e., 0.532 μm. The ZnSe sample was polycrystalline with random crystallite orientation and the observed second harmonic generation was angle insensitive though relatively inefficient. The threshold for visual detection (viewed through 1.06-μm laser safety goggles) of the second harmonic from the ZnSe was ~4 MW/cm^2. This is substantially below the intensity required to burn Polaroid film with 40-psec pulses. The relatively low threshold intensity for the generation of the second harmonic and the angle insensitivity make CVD ZnSe a relatively inexpensive, easy to use frequency doubling material where high efficiency is not needed. ZnSe thus makes a practical device for tracking and monitoring the presence of 1.06-μm beams.

IV. Summary

The laser-induced surface damage threshold was measured for the front surface of CdTe and other II–VI materials at a variety of pulse widths and focal spot radii at 1.06 μm. The results indicate that the damage threshold irradiance is independent of the focal radius and scales as $t_p^{-1/2}$. The observed surface damage in CdTe appears to be caused by linear absorption by surface defects and/or surface contaminants. Two-photon absorption and excess carrier absorption by the two-photon generated carriers were determined to be the dominant absorption mechanisms for CdTe and ZnTe and three-photon processes plus excess carriers were dominant for ZnSe and CdS. The depletion of the beam due to these nonlinear absorption processes prevented rear surface damage in all the specimens studied.

This work was supported by the office of Naval Research, the National Science Foundation (under grant ECS-8105513), The Robert A. Welch Foundation, and a Faculty Research grant from North Texas State University. The data on CdTe for 9-nsec pulses were taken at the Naval Weapons Center, China Lake, Calif. The authors acknowledge the help of J. B. Franck in setting up and characterizing the nanosecond laser used for this test and for assisting in the measurements. We also acknowledge the support of Dwight Maxon and H. J. Mackey for providing the data acquisition and microcomputer control system used in this work and Arthur L. Smirl for help in spectral emission measurements.

References

1. N. Bloembergen, Appl. Opt. **12,** 661 (1973).
2. P. A. Temple and M. J. Soileau, Natl. Bur. Stand. (U.S.) Spec. Publ. 462 (1976), p. 371.
3. J. R. Bettis, A. Guenther, and A. Glass, Natl. Burr. Stand. (U.S.) Spec. Publ. 414 (1974), p. 214.
4. C. C. Wang, Phys. Rev. B **2,** 2045 (1970).
5. R. Ozarski, Lawrence Livermore National Laboratory; private communication (1981).
6. Quantel model YG-40, 928 Benecia Avenue, Sunnyvale, Calif. 94086.
7. W. H. Glenn and M. J. Brienza, Appl. Phys. Lett. **10,** 221 (1967).
8. D. J. Bradley and G. H. C. New, Proc. IEEE **62,** 313 (1974).
9. E. W. Van Stryland, and M. A. Woodall in *Laser-Damage in Optical Materials: 1980*, Natl. Bur. Stand. (U.S.) Spec. Publ. 620 (1980), p. 50.
10. E. W. Van Stryland, M. A. Woodall, M. J. Soileau, and W. E. Williams, in *Proceedings, 1981 Conference on Laser-Induced Damage to Optical Materials, Boulder, Colo.* (National Bureau of Standards, Washington, D.C., 1982).
11. M. J. Soileau, Appl. Opt. **20,** 1030 (1981).
12. The ZnSe material was grown by the Raytheon Research Laboratories, Bedford, Mass. The CdTe was purchased from II–VI, Inc. Saxonburgh, Pa., and CdS and ZnTe were purchased from Cleveland Crystals, Cleveland, Ohio.
13. J. O. Porteus, J. L. Jernigan, and W. N. Faith, Natl. Bur. Stand. (U.S.) Spec. Publ. 509 (1977), p. 507.
14. M. D. Crisp, N. L. Boling, and G. Buge, Appl. Phys. Lett. **21,** 354 (1972).
15. J. H. Bechtel and W. L. Smith, Phys. Rev. B **12,** 3515 (1976).
16. F. Brynkner, V. S. Dneprovskii, and V. S. Khattaton. Sov. J. Quantum Electron. **4,** 6 (1975).
17. M. Bass, E. W. Van Stryland, and A. F. Stewart, Appl. Phys. Lett. **34,** 142 (1979).
18. R. H. Hellwarth, Natl. Bur. Stand. (U.S.) Spec. Publ. 341 (1970), p. 67.
19. M. J. Soileau, M. Bass, and P. H. Klein, Natl. Bur. Stand. (U.S.) Spec. Publ. 568 (1979), p. 497.
20. A. A. Barshch, M. S. Brodin, and N. N. Krupa. Sov. J. Quantum Electron. **7,** (9) 113 (1977).
21. J. R. Bettis, R. A. House II, and A. H. Guenther, Natl. Bur. Stand. (U.S.) Spec. Publ. 462 (1976), p. 338.
22. M. Sparks and C. D. Duthler, J. Appl. Phys. **44,** 3038 (1973).